INTERNATIONAL JOURNAL OF HYDROGEN ENERGY 35 (2010) 500–510

Available at www.sciencedirect.com

ScienceDirect

journal homepage: www.elsevier.com/locate/he

Maximizing the solar to H_2 energy conversion efficiency of outdoor photobioreactors using mixed cultures

Halil Berberoğlu [a,*], *Laurent Pilon* [b]

[a] *Mechanical Engineering Department, Cockrell School of Engineering, The University of Texas at Austin – Austin, TX 78712, USA*
[b] *Mechanical and Aerospace Engineering Department, Henry Samueli School of Engineering and Applied Science University of California, Los Angeles – Los Angeles, CA 90095, USA*

ARTICLE INFO

Article history:
Received 8 August 2009
Received in revised form
29 October 2009
Accepted 7 November 2009
Available online 24 November 2009

Keywords:
Algae
Purple bacteria
Photobioreactor
Photobiological hydrogen

ABSTRACT

A numerical study is presented aiming to maximize the solar to hydrogen energy conversion efficiency of a mixed culture containing microorganisms with different radiation characteristics. The green algae *Chlamydomonas reinhardtii* CC125 and the purple non-sulfur bacteria *Rhodobacter sphearoides* ATCC 49419 are chosen for illustration purposes. The previously measured radiation characteristics of each microorganism are used as input parameters in the radiative transport equation for calculating the local spectral incident radiation within a flat panel photobioreactor. The specific hydrogen production rate for each microorganism as a function of the available incident radiation is recovered from data reported in the literature.

The results show that for mono-cultures, the solar to H_2 energy conversion efficiency, for all combinations of microorganism concentrations and photobioreactor thicknesses, fall on a single line with respect to the optical thickness of the system. The maximum solar energy conversion efficiency of mono-cultures of *C. reinhardtii* and *R. spaheroides* are 0.061 and 0.054%, respectively, corresponding to optical thicknesses of 200 and 16, respectively. Using mixed cultures, a total conversion efficiency of about 0.075% can be achieved corresponding to an increase of about 23% with respect to that of a mono-culture of *C. reinhardtii*. It has been shown that the choice of microorganism concentrations for maximum solar energy conversion efficiency in mixed cultures is non-trivial and requires careful radiation transfer analysis coupled with H_2 production kinetics taking into account the photobioreactor thickness.

1. Introduction

Photobiological hydrogen production by cultivation of photosynthetic microorganisms in photobioreactors offers a clean and sustainable alternative to thermochemical or electrolytic hydrogen production technologies [1–3]. However, solar to hydrogen energy conversion efficiency of photobioreactors remain a major challenge [4–8].

This technology uses photosynthetic microorganisms such as green algae, cyanobacteria and purple non-sulfur bacteria to produce hydrogen from solar energy at mild temperatures and pressures [1,2]. Depending on the source of electrons, photobiological hydrogen production is classified under three categories [1,9–11]. In direct biophotolysis, electrons are directly derived from water splitting and used to reduce protons to hydrogen molecule with hydrogenase enzymes. On

* *Corresponding author*. Mechanical Engineering Department, Cockrell School of Engineering, The University of Texas at Austin - Austin, TX 78712, USA. Tel.: +1 512 232 8459; fax: +1 512 471 1045.
E-mail address: berberoglu@mail.utexas.edu (H. Berberoğlu).
0360-3199/$ – see front matter
doi:10.1016/j.ijhydene.2009.11.030

Nomenclature

$A_{abs,\lambda}$	spectral mass absorption cross-section of microorganisms, m^2/kg
$A_{abs,\lambda}$	spectral mass absorption cross-section, m^2/kg
A_s	irradiated surface area of the photobioreactor, m^2
$S_{sca,\lambda}$	spectral mass scattering cross-section, m^2/kg
G	incident radiation, W/m^2
g	Henyey-Greenstein asymmetry factor
H	irradiation, W/m^2
I_λ	spectral intensity, $W/m^2/sr/nm$
k	absorption index
K_G	saturation irradiation, W/m^2
K_I	inhibition irradiation, W/m^2
L	thickness of the photobioreactor, m
M	molecular mass, kg/mol
$\dot{m}_{H_2}$	total production rate of hydrogen, kg/h
P_o	total pressure, Pa
P_{H_2}	partial pressure of H_2, Pa
R	universal gas constant, $R = 8.314$ J/mol/K
$\hat{s}$	unit vector into a given direction
ν_X	specific volume of the microorganisms, m^3/kg
w_i	weights for the Gaussian quadrature
V_L	liquid volume in the photobioreactor, m^3
X	microorganism concentration, kg dry cell/m^3
z	distance from the illuminated surface, m

Greek symbols

α	threshold parameter
β	extinction coefficient, m^{-1}
ΔG^o	standard-state free energy of formation of H_2 from water splitting reaction, J/mol
η_{H_2}	solar to hydrogen energy conversion efficiency
θ	polar angle, rad
θ_i	discrete polar angles corresponding to the directions of the Gaussian quadrature, rad
Θ	angle between incident and scattered directions, rad
κ	absorption coefficient, m^{-1}
λ	wavelength, nm
π_{H_2}	specific hydrogen production rate, L/kg/h
σ	scattering coefficient, m^{-1}
τ	optical thickness
φ	azimuthal angle, rad
Φ	scattering phase function
Ω	solid angle, sr

Subscripts

A	refers to microorganism A
abs	refers to absorption
use	refers to useable incident radiation for producing hydrogen
B	refers to microorganism B
c	refers to collimated light
d	refers to diffuse light
eff	refers to effective radiation characteristics
H_2	refers to hydrogen
m	refers to medium
max	refers to maximum
λ	refers to wavelength
sat	refers to saturation incident radiation
sca	refers to scattering
tot	refers to total
z	refers to local values

the other hand, in indirect biophotolysis, the electrons from water splitting are first converted into organic molecules. These molecules are then degraded and the electrons are used by the hydrogenase and/or nitrogenase enzymes to reduce protons to hydrogen. Finally, in photofermentation electrons are derived from external organic matter found in the surrounding medium of the microorganisms.

Thus far, research efforts have mainly concentrated on cultivating single species of microogranisms for photobiological hydrogen production. Among these, cyanobacteria and green algae which utilize solar energy in the spectral range from 400 to 700 nm to produce hydrogen have been studied extensively [5,9,12–16]. Purple non-sulfur bacteria have also been identified as promising hydrogen producers which mainly use solar energy in the near-infrared part of the spectrum from 700 to 900 nm [17–21]. Note that only about 45% of the total solar radiation is emitted between 400 and 700 nm and an additional 20% is emitted between 700 and 900 nm [6,22].

Thus, hydrogen production from a mixed culture of green algae and purple bacteria has the potential to achieve higher solar to hydrogen energy conversion efficiencies than single cultures by using solar radiation in the spectral range from 400 to 900 nm representing about 65% of the total solar radiation [22]. One such mixed system was demonstrated by Melis and Melnicki [22] where the green algae *Chlamydomonas reinhardtii* were co-cultured with the purple bacteria *Rhodospirillum rubrum*. The authors suggested that once the photosynthesis to respiration (P/R) ratio of the green algae was reduced to 1, such a co-culture could be used for more efficient photobiological hydrogen production. Unfortunately, the purple bacteria also absorb light in the visible part of the spectrum due to the presence of bacteriochlorophyll b and carotenoids [23] and the species may compete for light during hydrogen production.

The productivity and the solar energy conversion efficiency of these systems depend on (i) light utilization by the different microorganisms and (ii) biological interactions between the two species. Biological interactions in mixed cultures are complex functions of culture conditions and species. In addition, photobiological hydrogen production is an enzymatic process which depends on temperature, pH, and composition of the culture medium as well as the concentrations of dissolved gas species such as oxygen, hydrogen, and nitrogen. To the best of our knowledge, no data or model is available in the literature to fully account for the effects of all these parameters on the photobiological hydrogen production rate. Moreover, before experimentally dealing with these complex biological interactions, the benefits of mixed cultures over mono-cultures can be assessed numerically by considering the most favorable biological conditions

to determine (i) the potential energy conversion improvement and (ii) how the concentration of each microorganism can influence the hydrogen production of the system. Thus, the objective of this study is to investigate the hydrogen production rate and solar to hydrogen energy conversion efficiency of such a mixed culture as a function of irradiance and concentration of each species assuming that each microorganism is producing hydrogen at its most favorable conditions other than the local available light. The green algae *C. reinhardtii* CC125 and the purple non-sulfur bacteria *R. sphearoides* ATCC 49419 are used as representative species of green algae and non-sulfur purple bacteria since their radiation characteristics were recently reported [23,24].

2. Analysis

Let us consider a plane-parallel photobioreactor of thickness L as illustrated in Fig. 1. In United States, the average latitude angle for the contiguous 48 states is about 37°, thus for maximum solar radiation inception, the photobioreactor is inclined at the latitude angle of 37° with respect to the zenith [25]. The reactor contains a mixture of microorganism A, namely *C. reinhardtii*, at concentration X_A and microorganism B, namely *R. sphaeroides*, at concentration X_B. Both X_A and X_B are expressed in kg dry cell/m^3. The reactor is illuminated with solar irradiation comprised of both a collimated and a diffuse component from the sun facing surface. As light penetrates into the photobioreactor, it is absorbed by the liquid phase and the microorganisms and scattered anisotropically by the microorganisms.

2.1. Assumptions

In order to make the problem mathematically trackable it is assumed that: (1) light transfer is one-dimensional as the system is symmetric in the plane of the photobioreactor, (2) the reactor is well mixed and microorganisms are uniformly distributed and randomly oriented in the reactor, (3) the reactor is continuously sparged with argon to prevent oxygen or hydrogen buildup, (4) the interfacial area of the bubbles is less then 450 m^{-1} so that their effect on light transfer is negligible [26], (5) the liquid phase is non-emitting, cold, weakly absorbing, and non-scattering, (6) both surfaces of the photobioreactor are treated with a non-reflective coating over the spectral range from 300 to 900 nm, (7) radiation incident on the back surface is negligible compared with the radiation incident on the sun facing surface. Note that the mass concentration to number concentration conversion factor for *C. reinhardtii* CC125 was reported to be 7.60×10^6 cells/kg dry weight [24]. For the maximum algae concentration used in this study, i.e., 32 kg/m^3, the corresponding volume fraction is 0.025. Finally, the size parameter $x = 2\pi a/\lambda$ ranges between 105 and 24 over the spectral region from 300 nm to 1300 nm for *C. reinhardtii*, approximated as spheres 10 μm in diameter. These values of volume fraction and size parameters ensure that independent scattering prevails based on the discussion in Ref. [27].

Moreover, this numerical study focuses on the use of mixed culture systems to maximize photobiological hydrogen production. Thus, it is further assumed that (8) the microorganisms are cultivated at optimum conditions separately with no carbon or nitrogen limitations and are mixed at different concentrations right before the hydrogen production phase, (9) the reactor is kept isothermal at 25 °C with the aid of an active temperature control, and thus (10) the specific hydrogen production rate π_{H_2} depends only on the light available to the microorganisms.

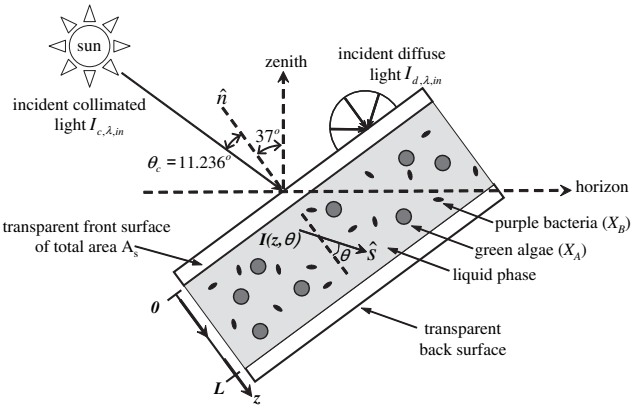

Fig. 1 – Schematic of the photobioreactor system considered. The boundary conditions correspond to 37° tilt sun facing surface for locations between latitudes 33°26′ and 46°52′ [25].

2.2. Governing equations and boundary conditions

The total intensity $I_\lambda(z,\hat{s})$ at a given location z in direction $\hat{s}$ is composed of a collimated and diffuse component, denoted by $I_{c,\lambda}(z,\hat{s})$ and $I_{d,\lambda}(z,\hat{s})$, respectively, and can be written as [28],

$$I_\lambda(z,\hat{s}) = I_{c,\lambda}(z,\hat{s}) + I_{d,\lambda}(z,\hat{s}) \quad (1)$$

The intensity I_λ can be determined by solving the radiative transfer equation (RTE) which is an energy balance on the radiative energy travelling along a particular direction $\hat{s}$. The steady-state RTE for the collimated intensity can be written as [28],

$$\frac{\partial I_{c,\lambda}(z,\hat{s})}{\partial z} = -\beta_{eff,\lambda} I_{c,\lambda}(z,\hat{s}) \quad (2)$$

where $\beta_{eff,\lambda}$ is the effective extinction coefficient expressed as,

$$\beta_{eff,\lambda} = \kappa_{eff,\lambda} + \sigma_{eff,\lambda} \quad (3)$$

where $\kappa_{eff,\lambda}$ and $\sigma_{eff,\lambda}$ are the effective linear absorption and scattering coefficients of the microorganism suspension in the photobioreactor expressed in m^{-1}. The effective absorption coefficient accounts for the absorption by the medium and by the microorganisms A and B at wavelength λ. Taking into account the volume fractions of microorganisms A and B in the photobioreactor given by $\nu_A X_A$ and $\nu_B X_B$, respectively, the effective absorption coefficient can be expressed as [29],

$$\kappa_{eff,\lambda} = \kappa_{m,\lambda}(1 - \upsilon_A X_A - \upsilon_B X_B) + A_{abs,\lambda,A} X_A + A_{abs,\lambda,B} X_B \quad (4)$$

where ν_A and ν_B are the specific volumes of microorganisms A and B, respectively, both assumed to be equal to 0.001 m^3/kg. The absorption coefficient of the medium $\kappa_{m,\lambda}$ is expressed in

m^{-1} and the mass absorption cross-sections of the microorganisms $A_{abs,\lambda,A}$ and $A_{abs,\lambda,B}$ are expressed in m^2/kg. Finally, the terms $A_{abs,\lambda,A}X_A$ and $A_{abs,\lambda,B}X_B$ correspond to the absorption coefficients of microorganisms *A* and *B*, respectively.

Similarly, the effective scattering coefficient of the co-culture $\sigma_{eff,\lambda}$ can be expressed as [29],

$$\sigma_{eff,\lambda} = \sigma_{\lambda,A} + \sigma_{\lambda,B} = S_{sca,\lambda,A}X_A + S_{sca,\lambda,B}X_B \tag{5}$$

where the coefficients $\sigma_{\lambda,A}$ and $\sigma_{\lambda,B}$ are the spectral scattering coefficients expressed in m^{-1} and $S_{sca,\lambda,A}$ and $S_{sca,\lambda,B}$ are the the mass scattering cross-sections of microorganism A and B, respectively, expressed in m^2/kg.

Moreover, considering the in-scattering by each species of microorganisms separately, the steady-state RTE for the diffuse intensity can be written as [28],

$$\frac{\partial I_{d,\lambda}(z,\hat{s})}{\partial z} = -\kappa_{eff,\lambda}I_{d,\lambda}(z,\hat{s}) - \sigma_{eff,\lambda}I_{d,\lambda}(z,\hat{s}) + \frac{\sigma_{eff,\lambda}}{4\pi}\int_{4\pi} I_{d,\lambda}(z,\hat{s}_i)\Phi_{eff,\lambda}(\hat{s}_i,\hat{s})d\Omega_i + \frac{\sigma_{eff,\lambda}}{4\pi}\int_{4\pi} I_{c,\lambda}(z,\hat{s}_i)\Phi_{eff,\lambda}(\hat{s}_i,\hat{s})d\Omega_i \tag{6}$$

where $\Phi_{eff,\lambda}$ is the effective scattering phase function microorganism mixture defined as [29],

$$\Phi_{eff,\lambda}(\hat{s}_i,\hat{s}) = \frac{\sigma_{\lambda,A}\Phi_{\lambda,A}(\hat{s}_i,\hat{s}) + \sigma_{\lambda,B}\Phi_{\lambda,B}(\hat{s}_i,\hat{s})}{\sigma_{\lambda,A} + \sigma_{\lambda,B}} \tag{7}$$

The scattering phase functions $\Phi_{\lambda,A}$ and $\Phi_{\lambda,B}$ for *C. reinhardtii* and *R. sphaeroides*, respectively, represent the probability that radiation travelling in the solid angle $d\Omega_i$ around the direction $\hat{s}_i$ will be scattered into the solid angle $d\Omega$ around direction $\hat{s}$. The first integral term in Equation (6) accounts for the in-scattered diffuse radiation whereas the second one corresponds to the in-scattered collimated radiation from an arbitrary direction $\hat{s}_i$ into the direction of interest $\hat{s}$.

Finally, the reactor is illuminated with solar radiation through transparent and non-reflecting window from the sun facing surface. In the case of the collimated radiation, the boundary conditions for Equation (2) can be written as,

$$\begin{aligned} I_{c,\lambda}(0,\theta) &= I_{c,\lambda,in}\delta(\theta-\theta_c) \quad \text{for } 0 \le \theta \le \pi \\ I_{c,\lambda}(L,\theta) &= 0 \quad \text{for } \pi \le \theta \le 2\pi \end{aligned} \tag{8}$$

where $I_{c,\lambda,in}$ is the intensity of the incident collimated terrestrial solar radiation, θ_c is the angle of the collimated sunlight with respect to the surface normal of the photobioreactor and $\delta(\theta-\theta_c)$ is the Kronecker delta function. Similarly, the diffuse component of the intensity in Equation (6) is given by,

$$\begin{aligned} I_{d,\lambda}(0,\theta) &= I_{d,\lambda,in} \quad \text{for } 0 \le \theta \le \pi \\ I_{d,\lambda}(L,\theta) &= 0 \quad \text{for } \pi \le \theta \le 2\pi \end{aligned} \tag{9}$$

where $I_{d,\lambda,in}$ is the incident diffuse terrestrial solar radiation. In this study, the values of the incident intensities were recovered from the spectral collimated irradiation denoted by $H_{c,\lambda}$ and the diffuse irradiation $H_{d,\lambda}$ according to,

$$I_{c,\lambda,in} = H_{c,\lambda} \text{ and } I_{d,\lambda,in} = \frac{H_{d,\lambda}}{2\pi} \tag{10}$$

where $H_{c,\lambda}$ and $H_{d,\lambda}$ are reported by Gueymard et al. [25] who used the code SMARTS [30] to calculate the spectral collimated and diffuse terrestrial solar irradiation [25]. The reported values correspond to a total solar irradiation of 1000 W/m^2 incident on a south facing surface with a 37° tilt with respect to the zenith. The angle of the sun is 48.236° with respect to the zenith and the air mass (AM), corresponding to the pathlength through the atmosphere relative to the zenith or overhead position, is equal to 1.5 for an observer at sea level. This value was selected to correspond to the AM value at locations between latitudes 46°52′ (Caribou, ME) and 33°26′ (Phoenix, AZ) where most of the solar energy conversion systems are located in the United States [25]. Under these conditions the angle of incidence of the collimated radiation denoted by θ_c corresponds to 11.236° with respect to the normal of the photobioreactor window and shown in Fig. 1. The total collimated and diffuse solar irradiation within the spectral range from 300 to 1300 nm, denoted by H_c and H_d are equal to 773 and 97 W/m^2, respectively.

2.3. Radiation characteristics of the medium and microorganisms

The radiation characteristics of the liquid medium were assumed to be those of pure water within the spectral region from 300 to 1300 nm. The spectral absorption coefficient of the medium is given by [31],

$$\kappa_{m,\lambda} = \frac{4\pi k_\lambda}{\lambda} \tag{11}$$

where k_λ is the absorption index of water reported by Hale and Querry [32].

The radiation characteristics of *C. reinhardtii* and *R. sphaeroides* was experimentally measured and reported by Berberoğlu and co-workers [23,24] in the spectral range from 300 to 1300 nm. In addition, the scattering phase function was assumed to be independent of wavelength in the same spectral range. Moreover, in an earlier study Berberoğlu et al. [26] showed that Henyey-Greenstein (HG) phase function gave satisfactory results for predicting local incident radiation in photobioreactors featuring high microorganism concentrations. The latter is given by [28],

$$\Phi_{HG,i}(\hat{s}_i,\hat{s}) = \frac{1-g_i^2}{\left[1+g_i^2-2g_i\cos\Theta\right]^{3/2}} \quad i = A \text{ or } B \tag{12}$$

where Θ is the scattering angle between directions $\hat{s}_i$ and $\hat{s}$ and g_i is the mean cosine of the scattering phase function for species *i*, also known as the Henyey-Greenstein asymmetry factor. HG phase function was used with the associated asymmetry factors of $g_A = 0.9834$ and $g_B = 0.9651$ for *C. reinhardtii* and for *R. sphaeroides*, respectively [23,24].

2.4. Method of solution

The overall numerical procedure is summarized in Fig. 2. First, Equation (2) was solved analytically subject to the boundary conditions expressed in Equation (8) to yield [28],

$$I_{c,\lambda}(z,\hat{s}) = I_{c,\lambda,in}\exp\left(-\frac{\beta_{eff,\lambda}z}{\cos\theta_c}\right)\delta(\hat{s},\hat{s}_c) \tag{13}$$

Then, Equation (6) was solved for $I_{d,\lambda}(z,\hat{s})$ using the discrete ordinates method [28] with a combination of two Gauss

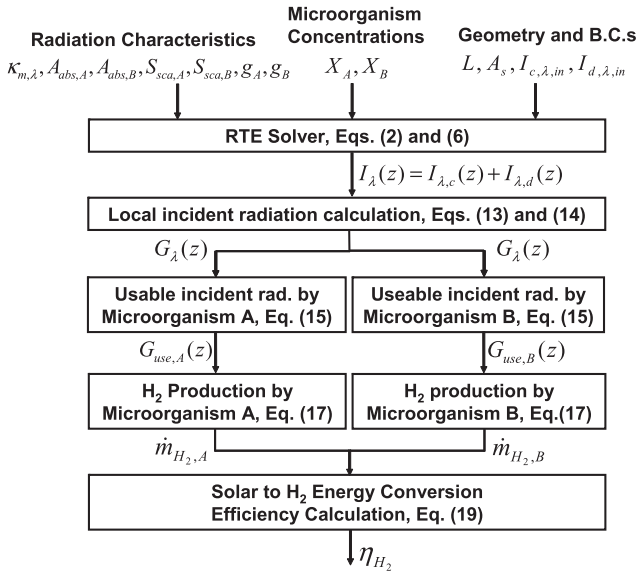

Fig. 2 – Schematic of the steady-state solution procedure.

quadrature having 24 discrete directions $(\Theta_i)_{1 \le i \le 24}$ per hemisphere along with the associated weighting factors w_i successfully used by Baillis et al. [33] for strongly forward scattering media.

Finally, the local spectral incident radiation was defined as [28],

$$G_\lambda(z) = \int_{4\pi} I_\lambda(z,\hat{s})\,d\Omega = 2\pi \sum_{i=1}^{24} w_i I_\lambda(z,\theta_i) \tag{14}$$

Convergence studies were performed to ensure that the computed values of $G_\lambda(z)$ were independent of both the grid size and the angular discretization. To do so, the number of grid points was doubled until the relative discrepancy between $G_\lambda(z)$ obtained for two consecutive grid refinements did not change by more than 1%. It was found that 1200 points along the z-direction satisfied this criterion for all microorganism concentrations explored. Moreover, the values of $G_\lambda(z)$ did not vary by more than 0.6% as the number of directions per hemisphere was increased from 24 to 30. The use of 24 directions is retained in the developed numerical tool to provide flexibility in incorporating other strongly forward scattering inclusions such as gas bubbles [26,33,34]. Finally, spectral simulations were performed from 400 to 1300 nm by increments of 5 nm corresponding to the spectral resolution of the experimental apparatus used by Berberoğlu and Pilon [23,24].

2.5. *Specific hydrogen production rates*

Algae and cyanobacteria contain pigments known as chlorophylls whereas purple bacteria contain bacteriochlorophylls along with accessory pigments such as carotenoids and phycobilin proteins in order to absorb and use the light energy to drive various biochemical reactions [35]. Therefore, it is not just the apparent absorption spectrum but specifically the absorption spectrum of these light harvesting pigments that are responsible for driving chemical reactions responsible for hydrogen production. In order to model the hydrogen production, the concept of useable incident radiation denoted by $G_{use}(z)$ is defined as,

$$G_{use}(z) = \int_0^\infty \alpha_\lambda G_\lambda d\lambda \tag{15}$$

where α_λ is the band parameter corresponding to the absorption band of the light harvesting pigments. For *C. reinhardtii* it is given by $\alpha_{\lambda,A} = 1$ for 350 nm $\le \lambda \le$ 710 nm corresponding to absorption by pigments such as chlorophyll a and b and carotenoids [35,36] while $\alpha_{\lambda,A} = 0$ for $\lambda <$ 350 nm and $\lambda >$ 710 nm. On the other hand, for *R. sphaeroides* $\alpha_{\lambda,B} = 1$ for 320 nm $\le \lambda \le$ 610 nm and for 760 nm $\le \lambda \le$ 910 nm corresponding to absorption by pigments such as bacteriochlorophyll b and carotenoids [35–37]. Outside these absorption bands, $\alpha_{\lambda,B}$ is equal to zero. Fig. 3 shows the absorption spectrum of *C. reinhardtii* and *R. sphaeroides* along with the corresponding α_λ.

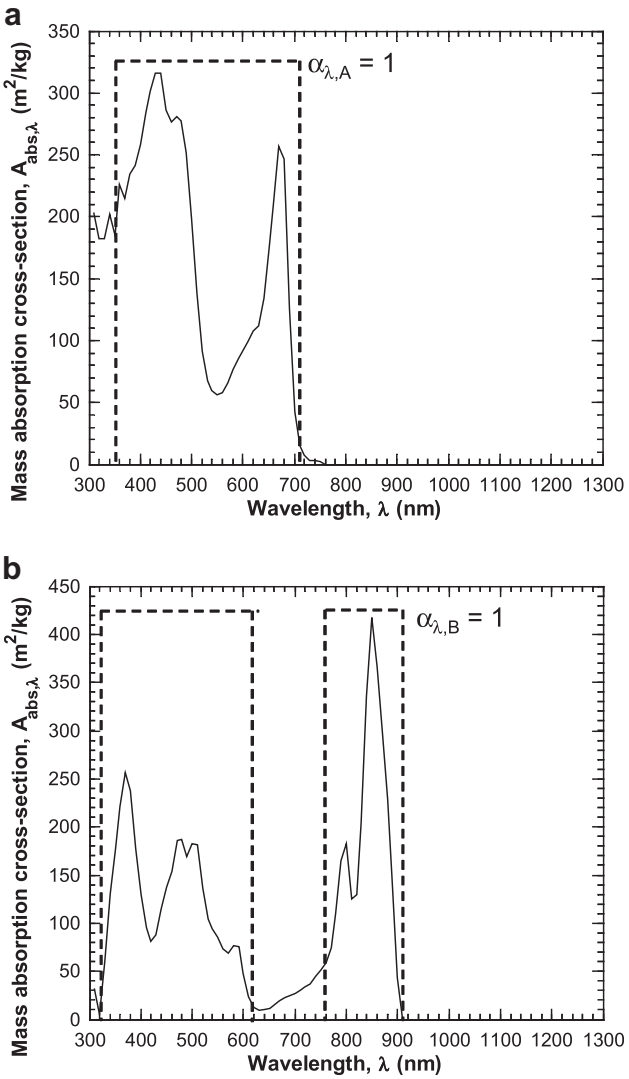

Fig. 3 – The absorption cross-section and the α_λ parameter of (a) *C. reinhardtii* CC125 [24] and (b) *R. sphaeroides* [23], respectively.

Nogi et al. [17] measured the specific hydrogen production rate π_{H_2} of the purple non-sulfur bacteria *Rhodopseudomonas rutila*. The authors reported the absorption spectrum, the hydrogen production rate as a function of spectral incident radiation, and the specific hydrogen production rate as a function of usable radiation. Due to the similarities in the absorption spectra and in the magnitude of their specific hydrogen production rates [17,23,38], the data for *R. rutila* was used to model the hydrogen production rate of *R. sphaeroides*. The specific production rate π_{H_2} has been modeled with a Michaelis–Menten type equation [39],

$$\pi_{H_2}(z) = \pi_{H_2,max}\frac{G_{use}(z)}{K_G + G_{use}(z) + G_{use}^2(z)/K_I} \quad (16)$$

where $\pi_{H_2,max}$ is the maximum specific hydrogen production rate expressed in kg H_2/kg dry cell/h, K_G is the saturation irradiation for hydrogen production expressed in W/m^2. The parameter K_I is the inhibition irradiation expressed in W/m^2 and it accounts for the inhibition of hydrogen production by excessive irradiation. The parameters $\pi_{H_2,max}$, K_G, and K_I were estimated by least squares fitting of the experimental data reported over the usable incident radiation range from 0 to 80 W/m^2 [17]. The values of $\pi_{H_2,max}$, K_G, and K_I were found to be 1.3×10^{-3} kg H_2/kg dry cell/h, 25 W/m^2, and 120 W/m^2, respectively. Fig. 4 compares the prediction of Equation (16) for π_{H_2} with data reported by Nogi et al. [17].

For *C. reinhardtii*, the values of K_G and K_I were assumed to be the same, whereas the maximum specific hydrogen production rate $\pi_{H_2,max}$ was obtained from the literature as 5.51×10^{-4} kg H_2/kg dry cell/h for sulphur deprived cells [40].

Finally, the hydrogen production rate for a given microorganism species i, where i = A or B, in the entire photobioreactor expressed in kg H_2/h is defined as,

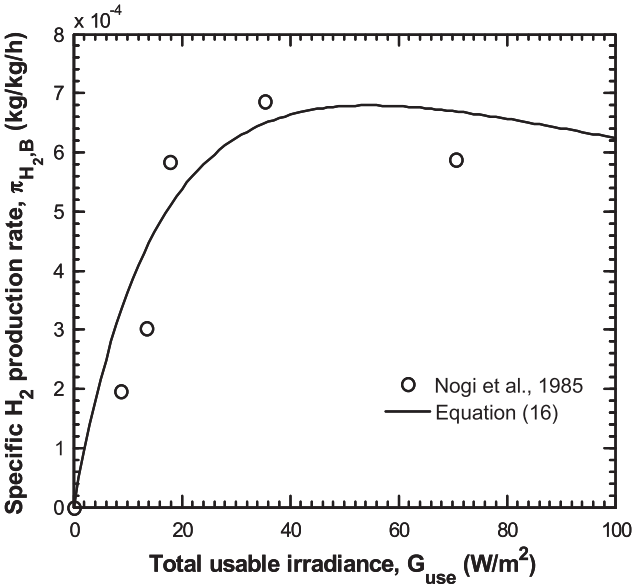

Fig. 4 – Experimental data [17] and the modified Michaelis–Menten model [Equation (16)] for the specific hydrogen production rate of *R. rutila* as a function of the usable incident radiation G_{use} with parameters $\pi_{H_2,max} = 1.3\times10^{-3}$ kg H_2/kg dry cell/h, K_G = 25 W/m^2, and K_I = 120 W/m^2.

$$\dot{m}_{H_2,i} = A_s \int_0^L \pi_{H_2,i}(z) X_i(z) dz \quad i = A \text{ or } B \quad (17)$$

where A_s is the surface area of the photobioreactor exposed to sunlight expressed in m^2 and $X_i(z)$ is the local concentration of species i. The total rate of hydrogen production $\dot{m}_{H_2}$ is the sum of the hydrogen production rate by the microorganism species A and B, i.e.,

$$\dot{m}_{H_2} = \dot{m}_{H_2,A} + \dot{m}_{H_2,B} \quad (18)$$

2.6. Light to hydrogen energy conversion efficiency

Finally, to compare different photobioreactor thicknesses and microorganism concentrations the light to hydrogen energy conversion efficiency of the mixed culture is defined as [41],

$$\eta_{H_2} = \frac{\Delta G_o \dot{m}_{H_2}}{M_{H_2} G_{in} A_s} \quad (19)$$

where G_{in} is the total solar irradiation equal to 1000 W/m^2, M_{H_2} is the molar mass of H_2 equal to 2.016×10^{-3} kg/mol and ΔG_o is the standard-state free energy of formation of H_2 from the water splitting reaction, equal to 236,337 J/mol at 303 K [42].

3. Results and discussion

Simulations were performed for four different values of photobioreactor thickness L, namely 1, 5, 10, and 20 cm. The concentration of *C. reinhardtii* X_A varied between 0.5 and 32 kg/m^3, and that of *R. sphaeroides* X_B varied between 0.05 and 1.0 kg/m^3. In all simulations the illuminated surface area of the photobioreactor A_s was taken as 1.0 m^2.

First, photobioreactors containing mono-cultures of *C. reinhardtii* and *R. sphaeroides* were considered. In order to assess the combined effect of different microorganism concentrations and photobioreactor thicknesses for mono-cultures, the total optical thickness is defined as [28],

$$\tau = \overline{\beta}_{eff} L \quad (20)$$

where $\overline{\beta}_{eff}$ is the effective extinction coefficient averaged over the spectral solar irradiation and is given by [28],

$$\overline{\beta}_{eff} = \frac{\int_0^\infty \beta_{eff,\lambda}(H_{c,\lambda} + H_{d,\lambda})d\lambda}{\int_0^\infty (H_{c,\lambda} + H_{d,\lambda})d\lambda} \quad (21)$$

where $\beta_{eff,\lambda}$ is given by Equation (3). The parameters τ and $\overline{\beta}_{eff}$ can be defined for each mono-culture.

Fig. 5(a) shows the solar to H_2 energy conversion efficiency $\eta_{H_2,A}$ and the hydrogen production rate $\dot{m}_{H_2,A}$ of the mono-culture of *C. reinhradtii* as a function of the optical thickness τ_A for all microorganism concentrations and values of photobioreactor thickness considered. It shows that the results for all microorganism concentrations and photobioreactor thicknesses fall on a single line and that the optical thickness defined above is an appropriate scale for assessing the performance of the photobioreactor containing a mono-culture of *C. reinhardtii*. Moreover, it shows that $\eta_{H_2,A}$ reaches a maximum of 0.061% corresponding to a H_2 production rate of 1.88×10^{-5} kg H_2/h at the optical thickness of about 200 for all cases. Note that the efficiency is small as G_{in} was computed

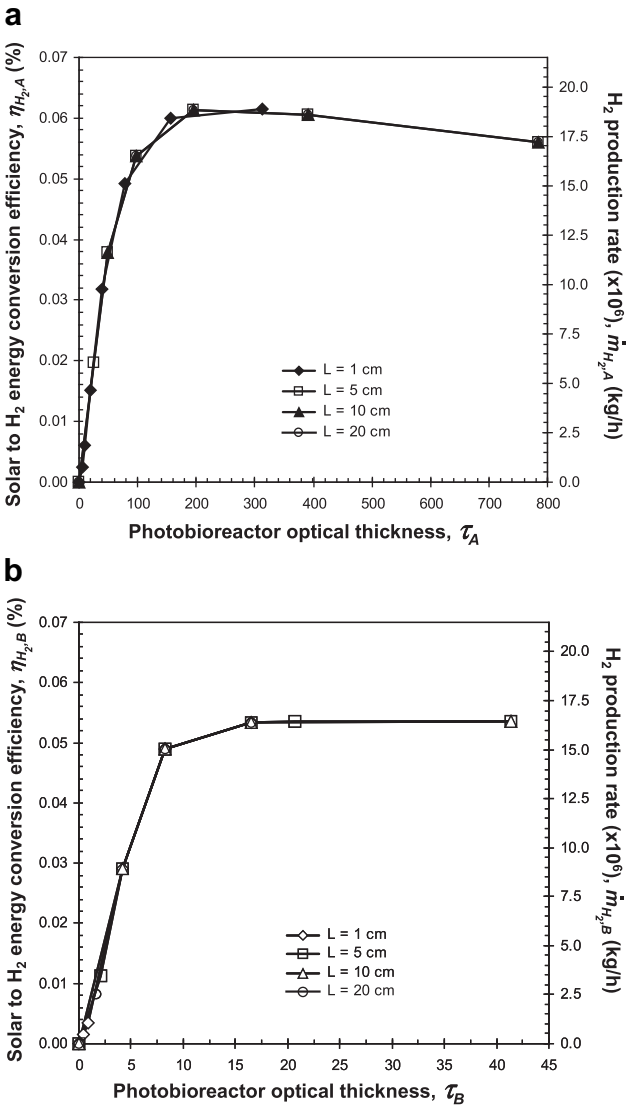

Fig. 5 – Solar to H_2 energy conversion efficiency and H_2 production rate per unit photobioreactor surface area for mono-cultures of (a) *C. reinhardtii* at X_A between 0.5 and 32 kg/m^3 and (b) *R. sphaeroides* at X_B between 0.05 and 1.0 kg/m^3 versus the photobioreactor optical thickness.

for the entire solar spectrum and not just the photo-active region. Table 1 shows the *C. reinhardtii* concentrations $X_{A,max}$ corresponding to an optical thickness of 200 for photobioreactor thickness equal to 1, 5, 10, and 20 cm. At optical thicknesses larger than 200, the efficiency decreases due to excessive absorption of light near the front surface resulting in limited light penetration into the reactor.

The order of magnitude of the solar to H_2 energy conversion efficiencies obtained from the simulations for *C. reinhardtii* is similar to that of the experimental data reported by Tsygankov et al. [42] for an outdoor photobioreactor which varied between 0.039 and 0.094%. The authors used the blue-green algae *Anabaena variabilis* PK84 at concentrations between 1.57 and 2.36 kg/m^3 in a 1 cm internal diameter helical photobioreactor operated outdoors with full sunlight.

Table 1 – *C. reinhardtii* $X_{A,max}$ and *R. sphaeroides* $X_{B,max}$ concentrations of mono- and mixed cultures for maximum solar to H_2 energy conversion efficiency $\eta_{H_2,max}$ and maximum H_2 production rate $\dot{m}_{H_2,max}$ for all photobioreactor thicknesses.

L (cm)	$\eta_{H_2,max}$ (%)	$\dot{m}_{H_2,max} \times 10^6$ (kg/h)	$X_{A,max}$ (kg/m^3)	$X_{B,max}$ (kg/m^3)
1	0.061	18.8	20	0
5	0.061	18.8	4	0
10	0.061	18.8	2	0
20	0.061	18.8	1	0
1	0.054	16.5	0	1.9
5	0.054	16.5	0	0.4
10	0.054	16.5	0	0.2
20	0.054	16.5	0	0.1
1	0.074	22.8	32	0.5
5	0.075	23.2	8	0.1
10	0.075	23.2	4	0.05
20	0.074	22.8	4	0.05

The temperature of the photobiorector was maintained between 23 and 28°C during operation.

Similarly, Fig. 5(b) shows $\eta_{H_2,B}$ and $\dot{m}_{H_2,B}$ of the *R. sphaeroides* mono-culture as a function of the optical thickness τ_B for different values of L. In this case $\eta_{H_2,B}$ had a maximum value of about 0.054% corresponding to the H_2 production rate of 1.65×10^{-5} kg H_2/h at the optical thickness of about 16 for all cases considered in this study. However, the efficiency in the case of *R. sphaeroides* did not decrease at larger optical thicknesses. Table 1 also summarizes the maximum *R. sphaeroides* concentration corresponding to the optical thickness of 16 for photobioreactor thickness equal to 1, 5, 10, and 20 cm.

In order to better understand the trends observed in Fig. 5 (a) and (b), let us consider the local hydrogen production rate in a photobioreactor. Fig. 6 shows the local hydrogen production rate per cubic meter of a 5 cm thick reactor

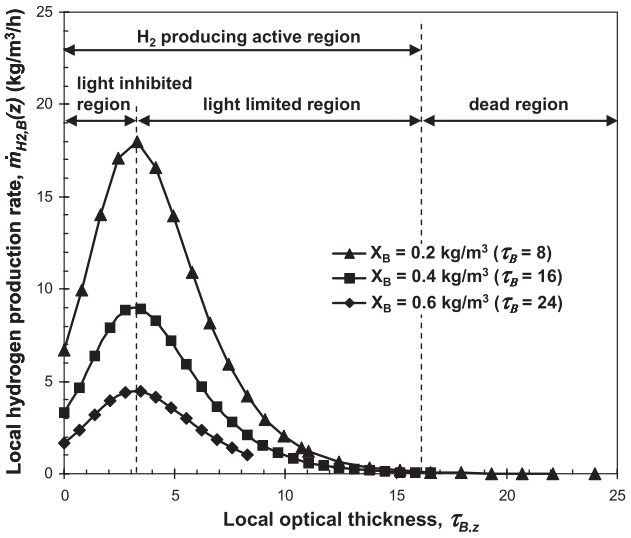

Fig. 6 – Light inhibited, light limited, and dead regions as a function of the local optical thickness for mono-cultures of *R. sphaeroides* with concentrations X_B equal to 0.2, 0.4, and 0.6 kg/m^3 in a 5 cm thick photobioreactor.

containing a mono-culture of *R. sphaeroides* at concentrations X_B equal to 0.2, 0.4 and 0.6 kg/m^3 as a function of the local optical thickness $\tau_{B,z}$. It indicates that the photobioreactor can be divided in three regions, namely (i) a light inhibited region where the local irradiation is so large that it reduces the local H_2 production rate, (ii) a light limited region where the local irradiation is small and hydrogen production cannot take place at its maximum capacity, and (iii) a dead region where local irradiation is so small that no hydrogen can be produced. The maximum hydrogen production rate is achieved at the local optical thickness $\tau_{B,z}$ of about 3.2 for all concentrations. For large enough concentrations, the local incident irradiation reaches such small values deep in the photobiroeactor that the production rate can vanish as in the case for local optical thicknesses larger than 16. The local hydrogen production rate integrated over the depth and multiplied by the cross-sectional area of the photobioreactor corresponds to the total hydrogen production rate presented in Fig. 5.

Similarly, Fig. 7 (a) shows the local production rate of hydrogen for the mono-culture of *C. reinhardtii* in a 5 cm thick photobioreactor as a function of the distance from the front surface. The results are shown for *C. reinhardtii* concentrations of 2, 4, and 16 kg/m^3 which correspond to an optical thickness of 100, 200, and 800, respectively. At relatively low microorganism concentrations corresponding to optical thicknesses τ_A less than 200, there was no dead region in the photobioreactor. However, as optical thickness increased to values larger than 200 the volume of dead region started increasing. Maximum total H_2 production rate was achieved for the largest microorganism concentration with no dead region in the photobioreactor. As previously discussed, this occurred at the optical thickness of 200 for *C. reinhardtii*. Further increase in microorganism concentration increased the volume of dead region, decreased the volume of light inhibited region and light limited region dominated. The increase in local peak production rate was outweighed by the decrease due to light limitation and increasing volume of dead region. Thus, the total rate of production decreased.

Furthermore, Fig. 7 (b) shows the local production rate of hydrogen for the mono-culture of *R. sphaeroides* in a 5 cm thick photobioreactor as a function of the distance from the illuminated surface. The results are shown for *R. sphaeroides* concentrations of 0.2, 0.4, and 0.8 kg/m^3 which correspond to an optical thickness τ_B of 8, 16, and 32, respectively. The maximum microorganism concentration where no dead region is present occurs at the optical thickness of 16. For larger optical thicknesses ($\tau_B = 32$), there was still a relatively thick light inhibited region and the active region was not dominated by the light limitation unlike for *C. reinhardtii*. Thus, the decrease in hydrogen producing volume is compensated by the increase in local production rate within the active region, resulting in a plateau in the total hydrogen production rate (Fig. 5).

Moreover, Fig. 8 (a)through (d) shows the total efficiency η_{H_2} and the total H_2 production rate $\dot{m}_{H_2}$ for mixed cultures of *C. reinhardtii* and *R. sphaeroides* for photobioreactor thicknesses of 1, 5, 10, and 20 cm, respectively. Due to strong differences in the absorption and scattering cross-sections of the microorganisms, the effective optical thickness of the mixed culture defined by Equations (20) and (21) failed to capture unified

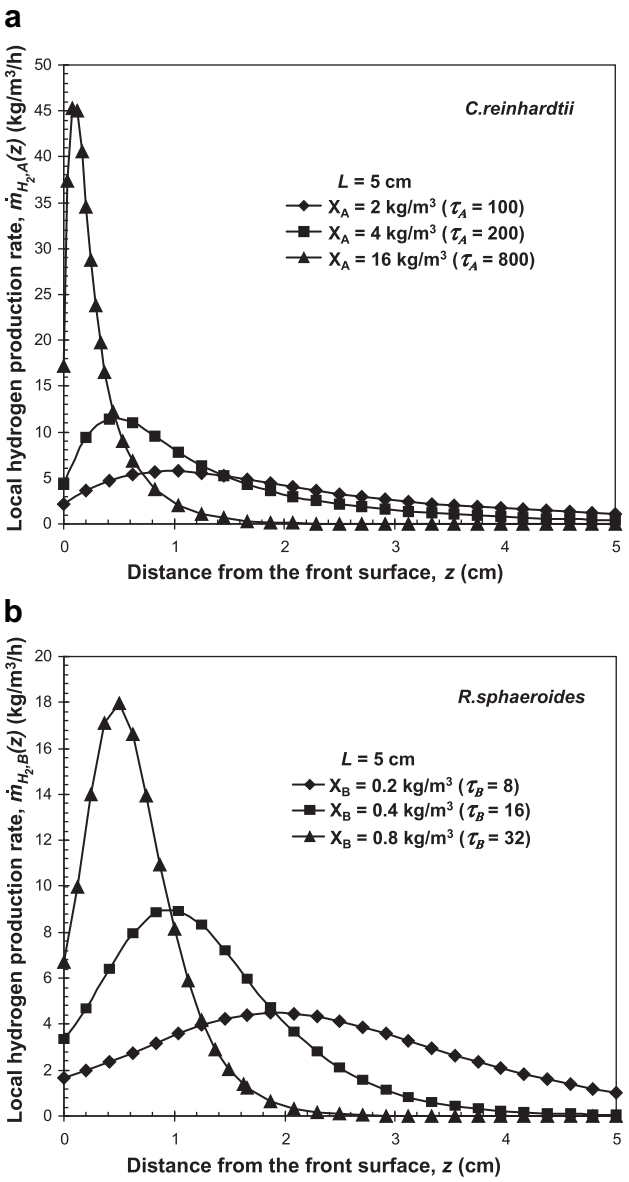

Fig. 7 – Local H_2 production rate as a function of the distance from the front surface for mono-cultures of (a) *C. reinhardtii* and (b) *R. sphaeroides* for a 5 cm thick photobioreactor.

trends. Thus, the results for mixed cultures are presented as a function of the *C. reinhardtii* concentrations for various concentrations of *R. sphaeroides*.

For a 1 cm thick photobioreactor, Fig. 8 (a)shows that a maximum efficiency of 0.074% was achieved for the mixed culture containing *C. reinhardtii* at a concentration of 32 kg dry cell/m^3 and *R. sphaeroides* at 0.5 kg dry cell/m^3. It corresponds to a hydrogen production rate of 2.27×10^{-5} kg H_2/h. This represents an increase in efficiency by 21% with respect to the maximum efficiency of a *C. reinhardtii* mono-culture. Further increase in *R. sphaeroides* concentration reduced the efficiency of the mixed culture. For 1 cm thick photobioreactor, *C. reinhardtii* concentrations larger than 32 kg dry cell/m^3 were not considered as such concentrations are not commonly reported in literature.

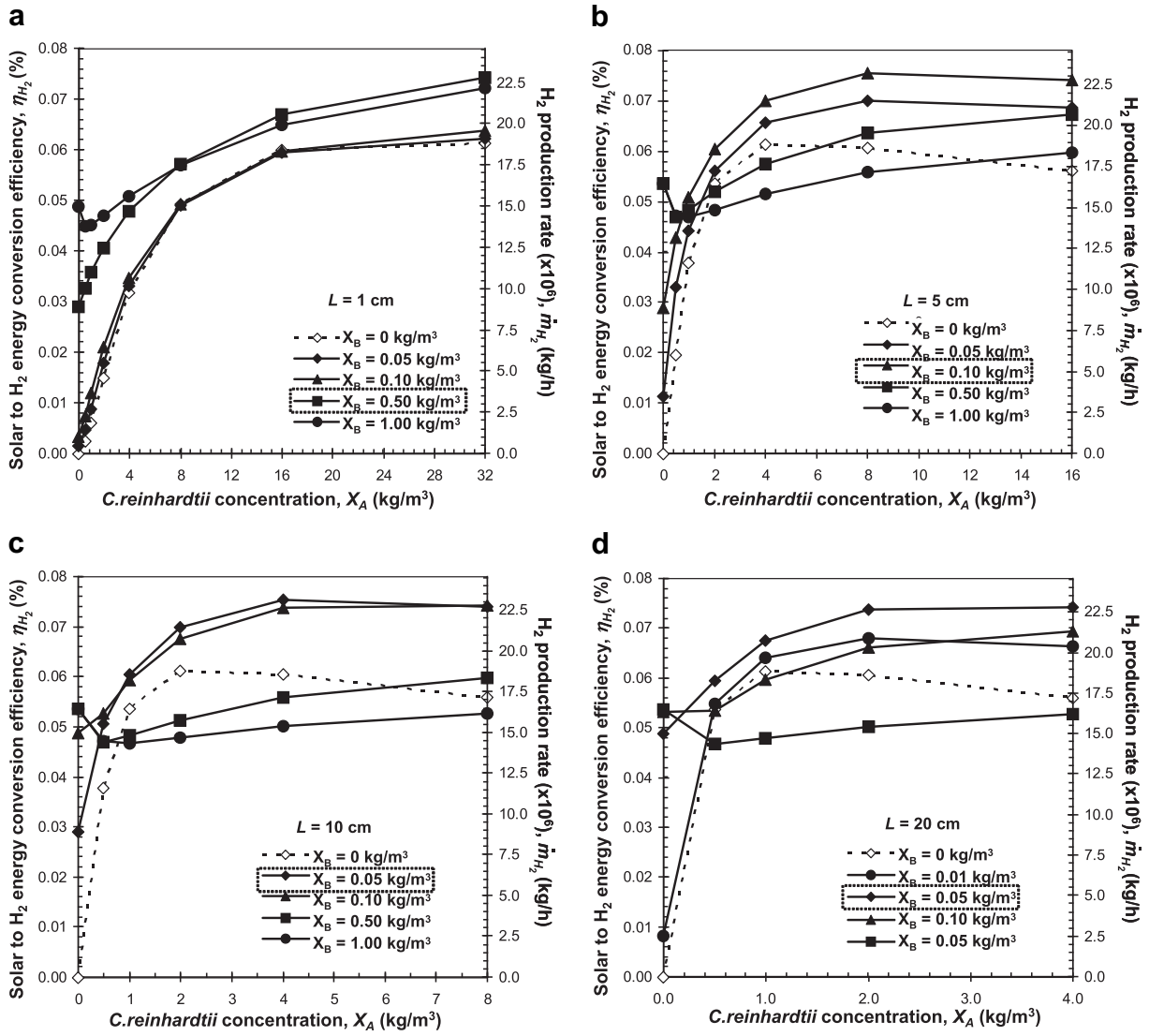

Fig. 8 – Solar to H_2 energy conversion efficiency and H_2 production rate of mixed cultures of *C. reinhardtii* (X_A) and *R. sphaeroides* (X_B) for (a) 1 cm, (b) 5 cm, (c) 10 cm, and (d) 20 cm thick photobioreactors.

Fig. 8 (b)shows that for a 5 cm thick photobioreactor, the efficiency reached up to 0.075% for the mixed culture containing 8 kg dry cell/m^3 of *C. reinhardtii* and 0.1 kg dry cell/m^3 *R. sphaeroides* corresponding to 2.30×10^{-5} kg H_2/hr. This represents an increase of 23% with respect to the maximum efficiency of a mono-culture of *C. reinhardtii* and an increase of 25% with respect to the efficiency of a mono-culture of *C. reinhardtii* at 8 kg dry cell/m^3. Further increase in either microorganism concentrations decreased the overall system performance. Trends similar to those obtained for 1 and 5 cm thick photobioreactors were also observed for 10 and 20 cm thick photobioreactors. The results are summarized in Table 1.

These results indicate that the choice of X_A and X_B for maximum solar energy conversion efficiency in mixed cultures is not trivial and requires careful radiation transfer analysis coupled with H_2 production kinetics taking into account the photobioreactor thickness. In addition, both microorganisms must be able to achieve their maximum performance in the same medium. This aspect, however, falls outside the scope of this study.

4. Conclusion

This study presented, for the first time, (i) an empirical model for photobiological hydrogen production and (ii) a numerical tool to determine the microorganism concentrations for maximizing the solar to H_2 energy conversion efficiency of mixed cultures of microorganisms having different radiation characteristics. The efficiency for the mono-culture of *C. reinhardtii* is of the same order of magnitude as that reported for an outdoor photobioreactor of similar dimensions [42]. The following conclusions can be drawn,

1. For mono-cultures, the performance of the reactor depends solely on the optical thickness of the system.

2. For a mono-culture of *C. reinhardtii* maximum solar to H_2 energy conversion efficiency of 0.061% is achieved for photobioreactor optical thickness τ_A equal to 200.
3. For a mono-culture of *R. spaheroides* maximum solar to H_2 energy conversion efficiency of 0.054% is achieved for photobioreactor optical thickness τ_B larger than 16.
4. For mixed cultures, a maximum solar to H_2 conversion efficiency of 0.075% can be achieved, corresponding to an increase of about 23% from the mono-culture of *C. reinhardtii*. The concentrations of *C. reinhardtii* and *R. sphaeroides* corresponding to this maximum efficiency depend on the thickness of the photobioreactor and can be found after careful analysis of radiation transfer and H_2 production kinetics.

Due to lack of empirical data, the photobiological hydrogen production has been modeled to be a sole function of spectral irradiation in this study. In order to expand the applicability of the presented tool, future work should focus on developing more advanced empirical models for photobiological hydrogen production taking into account the effects of temperature, pH, substrate availability and other complex biological interactions of green algae and purple non-sulfur bacteria. Then, these models can be readily integrated with the presented numerical tool. Moreover, using an appropriate kinetic moel, this tool can also be used for simulating other photobiological or photochemical process involving more than one species with different radiation characteristics or multiple photocatalysts with different band gaps.

REFERENCES

[1] Das D, Veziroğlu TN. Hydrogen production by biological processes: a survey of literature. International Journal of Hydrogen Energy 2001;26(1):13–28.
[2] Kovacs KL, Maroti G, Rakhely G. A novel approach for biohydrogen production. International Journal of Hydrogen Energy 2006;31:1460–8.
[3] Kalinci Y, Hepbasli A, Dincer I. Biomass-based hydrogen production: a review and analysis. International Journal of Hydrogen Energy 2009;34(21):8799–817.
[4] Hallenbeck PC, Benemann JR. Biological hydrogen production; fundamentals and limiting processes. International Journal of Hydrogen Energy 2002;27(11–12):1185–93.
[5] Melis A. Green alga hydrogen production: process, challenges and prospects. International Journal of Hydrogen Energy 2002;27(11–12):1217–28.
[6] Akkerman I, Jansen M, Rocha J, Wijffels RH. Photobiological hydrogen production: photochemical efficiency and bioreactor design. International Journal of Hydrogen Energy 2002;27(11–12):1195–208.
[7] Levin DB, Pitt L, Love M. Biohydrogen production: prospects and limitations to practical application. International Journal of Hydrogen Energy 2004;29(2):173–85.
[8] Das D. Advances in biohydrogen production processes: an approach towards commercialization. International Journal of Hydrogen Energy 2009;34(17):7349–57.
[9] Melis A, Happe T. Hydrogen production. Green algae as a source of energy. Plant Physiology 2001;127(3):740–8.
[10] Prince RC, Kheshgi HS. The photobiological production of hydrogen: potential efficiency and effectiveness as a renewable fuel. Critical Reviews in Microbiology 2005;31(1):19–31.
[11] Benemann JR. Hydrogen production by microalgae. Journal of Applied Phycology 2000;12(3–5):291–300.
[12] Pinto FAL, Troshina O, Lindblad P. A brief look at three decades of research on cyanobacterial hydrogen evolution. International Journal of Hydrogen Energy 2002;27(11–12): 1209–15.
[13] Yoon JH, Sim SJ, Kim MS, Park TH. High cell density culture of *Anabaena variabilis* using repeated injections of carbon dioxide for the production of hydrogen. International Journal of Hydrogen Energy 2002;27(11–12):1265–70.
[14] Liu J, Bukatin VE, Tsygankov AA. Light energy conversion into H_2 by *Anabaena variabilis* mutant PK84 dense cultures exposed to nitorgen limitation. International Journal of Hydrogen Energy 2006;31(11):1591–6.
[15] Laurinavichene TV, Fedorov AS, Ghirardi ML, Seibert M, Tsygankov AA. Demonstration of sustained hydrogen production by immobilized, sulfur-deprived *Chlamydomonas reinhardtii* cells. International Journal of Hydrogen Energy 2006;31(5):659–67.
[16] Winkler M, Hemschemeier A, Gotor C, Melis A, Happe T. [Fe]-hydrogenases in green algae: photo-fermentation and hydrogen evolution under sulfur deprivation. International Journal of Hydrogen Energy 2002;27(11–12):1431–9.
[17] Nogi Y, Akiba T, Horikoshi K. Wavelength dependence of photoproduction of hydrogen by *Rhodopseudomonas rutila*. Agricultural and Biological Chemistry 1985;49(1):35–8.
[18] Fascetti E, D'Addario E, Todini O, Robertiello A. Photosynthetic hydrogen evolution with volatile organic acids derived from the fermentation of source selected municipal solid wastes. International Journal of Hydrogen Energy 1998;23(9):753–60.
[19] Zhu H, Suzuki T, Tsygankov AA, Asada Y, Miyake J. Hydrogen production from tofu wastewater by *Rhodobacter sphaeroides* immobilized in agar gels. International Journal of Hydrogen Energy 1999;24(4):305–10.
[20] Kondo T, Arakawa M, Wakayama T, Miyake J. Hydrogen production by combining two types of photosynthetic bacteria with different characteristics. International Journal of Hydrogen Energy 2002;27(11–12):1303–8.
[21] Asada Y, Ohsawa M, Nagai Y, Ishimi K, Fukatsu M, Hideno A, et al. Re-evaluation of hydrogen productivity from acetate by some photosynthetic bacteria. International Journal of Hydrogen Energy 2008;33(19):5147–50.
[22] Melis A, Melnicki M. Integrated biological hydrogen production. International Journal of Hydrogen Energy 2006; 31(11):1563–73.
[23] Berberoğlu H, Pilon L. Experimental measurement of the radiation characteristics of *Anabaena variabilis* ATCC 29413-U and *Rhodobacter sphaeroides* ATCC 49419. International Journal of Hydrogen Energy 2007;32(18):4772–85.
[24] Berberoğlu H, Melis A, Pilon L. Radiation characteristics of *Chlamydomonas reinhardtii* CC125 and its truncated chlorophyll antenna transformants *tla1, tlaX*, and *tla1*-CW^+. International Journal of Hydrogen Energy 2008;33(22): 6467–83.
[25] Gueymard CA, Myers D, Emery K. Proposed reference irradiance spectra for solar energy system testing. Solar Energy 2002;73(6):443–67.
[26] Berberoğlu H, Yin J, Pilon L. Simulating light transfer in a bubble sparged photobioreactor for simultaneous hydrogen fuel production and CO_2 mitigation. International Journal of Hydrogen Energy 2007;32(13):2273–85.
[27] Tien CL, Drolen BL. Thermal radiation in particulate media with dependent and independent scattering. In: Chawla TC, editor. Annual review of numerical fluid mechanics and heat transfer, vol. 1. New York, NY: Hemisphere; 1987. p. 1–32.
[28] Modest MF. Radiative heat transfer. San Diego, CA: Academic Press; 2003.

[29] Lee SC, White S, Grzesik JA. Effective radiative properties of fibrous composites containing spherical particles. International Journal of Thermophysics and Heat Transfer 1994;8(3):400–5.
[30] Gueymard C. SMARTS, http://rredc.nrel.gov/solar/models/SMARTS/ [accessed on July 8, 2007].
[31] Bohren CF, Huffman DR. Absorption and scattering of light by small particles. New York: John Wiley & Sons; 1998.
[32] Hale GM, Querry MR. Optical constants of water in the 200-nm to 200-μm wavelength region. Applied Optics 1973;12(3):555–63.
[33] Baillis D, Pilon L, Randrianalisoa H, Gomez R, Viskanta R. Measurements of radiation characteristics of fused quartz containing bubbles. Journal of Optical Society of America 2004;21(1):149–59.
[34] Randrianalisoa H, Baillis D, Pilon L. Improved inverse method for radiative characteristics of closed-cell absorbing porous media. Journal of Thermophysics and Heat Transfer 2006;20(4):871–83.
[35] Madigan MT, Martinko JM. Biology of microorganisms. Upper Saddle River, NJ: Pearson Prentice Hall; 2006.
[36] Ke B. Photosynthesis, photobiochemistry and photobiophysics. Dordrecht, The Netherlands: Kluwer Academic Publishers; 2001.
[37] Broglie RM, Hunter CN, Delepelaire P, Niederman RA, Chua NH, Clayton RK. Isolation and characterization of the pigment-protein complexes of *Rhodopseudomonas sphaeroides* by lithium dodecylsulfate/polyacrylamide gel electrophoresis. Proceedings of the National Academy of Sciences of the United States of America 1980;77(1):87–91.
[38] Sasikala K, Ramana CV, Rao PR. Environmental regulation for optimal biomass yield and photoproduction of hydrogen by *Rhodobacter sphaeroides* O.U. 001. International Journal of Hydrogen Energy 1991;16(9):597–601.
[39] Dunn IJ, Heinzle E, Ingham J, Prenosil JE. Biological reaction engineering; dynamic modelling fundamentals with simulation examples. 2nd ed. Wiley-VCH; 2003.
[40] Laurinavichene T, Tolstygina I, Tsygankov A. The effect of light intensity on hydrogen production by sulphur-deprived Chlamydomonas reinhardtii. Journal of Biotechnology 2004;114(1–2):143–51.
[41] Bolton JR. Solar photoproduction of hydrogen, IEA Technical Report, IEA/H2/TR-96; 1996.
[42] Tsygankov AA, Fedorov AS, Kosourov SN, Rao KK. Hydrogen production by cyanobacteria in an automated outdoor photobioreactor under aerobic conditions. Biotechnology and Bioengineering 2002;80(7):777–83.